

# Comparative Study between Two- and Three-Dimensional Analyses of a Deep Excavation

Maria Spanea and Nikos Gerolymos

Geotechnical Department, School of Civil Engineering, National Technical University of Athens, GR-15780, Athens, Greece

Email: marspan53@gmail.com, gerolymos@gmail.com

**Abstract**—The subsoil stratigraphy, the excavation geometry, and the temporary supporting system are significant factors that affect the design and construction of a deep excavation. This paper presents the findings of a numerical simulation of an anchored pile-supported 36m deep excavation with a length to width ratio of  $L/B=2.2$ . The significance of 3D geometry and excavation stages in the out of plane direction on the pile wall's performance is highlighted. The analysis is carried out with PLAXIS FE code and the effective stress approach. The following critical parameters are used for the results' comparison: (a) wall lateral displacement, (b) ground settlement, and (c) internal structural forces. The impact of wall structural anisotropy and construction sequence on the soil-structure system's performance is also investigated. The unrealistic 2D boundary conditions considerably overestimate results in terms of both displacements and stresses of the wall, which may lead to an overconservative design.

**Index Terms**—Deep excavation, 3D finite element analyses, Structural anisotropy of pile wall

## I. INTRODUCTION

Underground structures have increased the recent years and especially metro stations in capital cities. Deep excavations are demanding technical projects, as their design and construction depend on various factors such as project location, supporting system and interaction with adjacent buildings that may settle due to ground excavation. During the last two decades, a considerable number of studies [1], [2], [3], [4] has been devoted to this subject using both 2D and 3D models for the numerical simulation of the excavation process. However, two-dimensional analyses for excavations with length to width ratio lower than six ( $L/B < 6$ ) are proved insufficient as they lead to over conservative design. In this study, the examined excavation is 36m deep, 20m wide and 44.2m long ( $L/B$  ratio equals to 2.2). The emphasis is on the role of 3D geometry, wall structural anisotropy and excavation progress in the out of plane direction on the wall performance. All numerical analyses were performed with the use of the Finite Element code PLAXIS. The results of finite element numerical analyses in two (2) and three (3) dimensions are compared in

terms of ground settlement, wall lateral displacement, and internal structural forces.

## II. PROBLEM DEFINITION

The studied problem refers to an excavation with length  $L=44.2\text{m}$ , width  $B=20.0\text{m}$  and depth  $D=36.0\text{m}$ . The geometry of the excavation and the excavation's phases are presented in the plan view and cross-section A-A' of "Fig. 1". The temporary supporting system includes a pile wall and twelve (12) rows of pre-stressed anchors. In specific, the pile wall is constructed of sixty-four (64) piles of 0.8m diameter up to 41m depth. Each of the short sides of the excavation ( $B=20\text{m}$ ) has ten (10) piles placed in axial distance 1.85m, whereas each of the long sides ( $L=44.2\text{m}$ ) has twenty-two (22) piles placed in axial distance 1.94m. The material used is concrete of C20/25 quality reinforced with B500c steel bars. Each pile is reinforced with fourteen (14) steel bars of  $\Phi 22$  diameter.

The excavation is performed in twelve (12) phases of 3m depth and pre-stressed anchors are constructed in each excavation phase. The anchors are placed 1m higher than the elevation of each excavation phase and have a downwards inclination of ten degrees ( $10^\circ$ ) with the horizontal plane. The grouted length equals to 12m for all anchors, whereas the free length is determined from the considered slipping surfaces. For the design of the free length, two different slipping surfaces were assumed with 30m and 44m depth, respectively, and an angle of  $45^\circ + (\phi/2) = 63^\circ$  with the horizontal plane. In that way, it is assumed that failure will occur due to sliding of the soil masses along the considered slipping surfaces. For that reason, the pre-stressed anchors should be grouted outside of the considered slipping surfaces. According to this limitation, it is geometrically proven that the upper five (5) rows of anchors should have a free length varying from 7.5m to 13.5m, whereas the free length of the lower seven (7) rows should vary from 9.9m to 18.9m. Additionally, the pre-stress force applied in each anchor of the first five (5) rows equals to 500 kN and the free length of the anchors contains four (4) steel tendons of  $\Phi 0.6''$  diameter with total area of  $5.6\text{cm}^2$ .

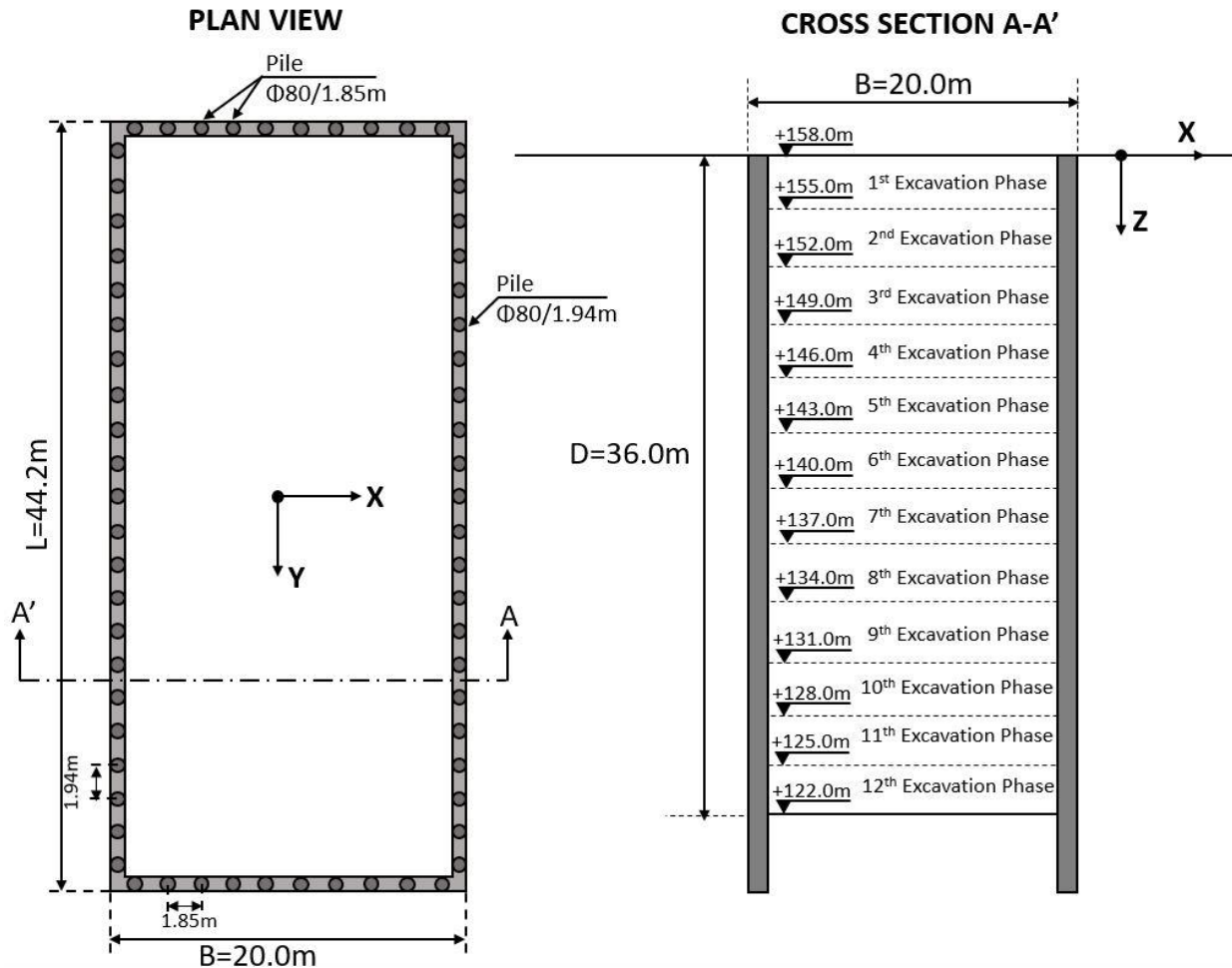


Figure 1. Plan view and cross section A-A' of the examined deep excavation.

The lower seven (7) rows have 6 steel tendons of  $\Phi 0.6''$  diameter which results to a total area of  $8.4\text{cm}^2$  and are pre-stressed with 700kN. The following Table I presents the properties of the pre-stressed anchors such as the grouted and free length, the total area of the steel tendons, the tension strength against yielding of the steel tendons and the applied pre-stress force for each row. The stratigraphy of the encountered soil layers is presented in “Fig. 2”. The considered values of the mechanical properties are mentioned in “Fig. 2” for each soil layer and are then used in the numerical analyses. Layer I is encountered from the ground surface up to 19m depth and from 29m to 36.6m depth. The upper soil Layer I is characterized as clay of low plasticity and clayey, sandy gravels. Layer II is encountered from 19m to 29m and from 36.6m to 44m depth. Layer II is characterized as conglomerate and is mainly found as a rocky formation. The lower Layer III is encountered lower than 44m and is a rocky formation characterized as schist. Regarding water presence in the subsoil, it is assumed that no groundwater level is formed at the region of the examined excavation. All soil layers are considered as drained. Layer I is numerically simulated using Hardening Soil Model Small Strain (HS small), whereas for Layer II and III the Mohr-Coulomb and Linear Elastic models are used, respectively.

TABLE I. PROPERTIES OF THE PRE-STRESSED GROUND ANCHORS

Ground Anchors Row	Free Length	Grouted Length	Section Area	Tension Strength	Pre-stress Force
	(m)	(m)	A(cm <sup>2</sup> )	(kN)	(kN)
1 <sup>st</sup>	13.5	12	5.6	952	500
2 <sup>nd</sup>	12.0	12	5.6	952	500
3 <sup>rd</sup>	10.5	12	5.6	952	500
4 <sup>th</sup>	9.0	12	5.6	952	500
5 <sup>th</sup>	7.5	12	5.6	952	500
6 <sup>th</sup>	18.9	12	5.6	1428	700
7 <sup>th</sup>	17.4	12	8.4	1428	700
8 <sup>th</sup>	15.9	12	8.4	1428	700
9 <sup>th</sup>	14.4	12	8.4	1428	700
10 <sup>th</sup>	13.0	12	8.4	1428	700
11 <sup>th</sup>	11.4	12	8.4	1428	700
12 <sup>th</sup>	9.9	12	8.4	1428	700

<b>Ground Surface</b>		<b>+158.0</b>
<b>Layer I</b>	<b>Material Model: HS small</b> $\gamma_{sat}=22 \text{ kN/m}^3$ , $\phi=36^\circ$ , $c=30 \text{ kPa}$ , $\psi=5^\circ$ , $E_{50}=E_{oed}=30 \text{ MPa}$ , $E_{ur}=90 \text{ MPa}$ , $\nu=0.20$ , $m_{power}=0.5$ , $\gamma_{0.7}=2 \times 10^{-4}$ , $G_o^{ref}=360 \text{ MPa}$ , $R_{int}=0.80$	<b>+139.0</b>
<b>Layer II</b>	<b>Material Model: Mohr-Coulomb</b> $\gamma_{sat}=22.5 \text{ kN/m}^3$ , $\phi=30^\circ$ , $c=150 \text{ kPa}$ , $\psi=5^\circ$ , $E'=250 \text{ MPa}$ , $\nu=0.20$ , $R_{int}=0.80$	<b>+129.0</b>
<b>Layer I</b>	<b>Material Model: HS small</b> $\gamma_{sat}=22.5 \text{ kN/m}^3$ , $\phi=36^\circ$ , $c=30 \text{ kPa}$ , $\psi=5^\circ$ , $E_{50}=E_{oed}=30 \text{ MPa}$ , $E_{ur}=90 \text{ MPa}$ , $\nu=0.20$ , $m_{power}=0.5$ , $\gamma_{0.7}=2 \times 10^{-4}$ , $G_o^{ref}=360 \text{ MPa}$ , $R_{int}=0.80$	<b>+121.4</b>
<b>Layer II</b>	<b>Material Model: Mohr-Coulomb</b> $\gamma_{sat}=22.5 \text{ kN/m}^3$ , $\phi=30^\circ$ , $c=150 \text{ kPa}$ , $\psi=5^\circ$ , $E'=250 \text{ MPa}$ , $\nu=0.20$ , $R_{int}=0.80$	<b>+114.0</b>
<b>Layer III</b>	<b>Material Model: Linear Elastic</b> $\gamma_{sat}=24 \text{ kN/m}^3$ , $E'=216 \text{ GPa}$ , $\nu=0.20$ , $R_{int}=0.80$	<b>+108.0</b>

Figure 2. Subsoil stratigraphy and mechanical properties of soil layers.

### III. NUMERICAL SIMULATION

In this paper the following numerical analyses were performed using finite element software PLAXIS2D and PLAXIS3D:

- Two-dimensional numerical analysis,
- Three-dimensional numerical analysis with isotropic pile wall and uniform excavation in the out of plane direction y-y,
- Three-dimensional numerical analysis with anisotropic pile wall and uniform excavation in the out of plane direction y-y,
- Three-dimensional numerical analysis with anisotropic pile wall and excavation in two (2) stages in the out of plane direction y-y,
- Three-dimensional numerical analysis with anisotropic pile wall and excavation in four (4) stages in the out of plane direction y-y.

#### A. Finite Element Mesh

For the numerical simulation of the examined deep excavation the two-dimensional model of “Fig. 3” was considered. The lateral boundaries are placed in distance 5B (which is equal to 100m) from the excavation’s sides. As a result, the total width of the numerical model is 220m. The lower boundary is placed at 50m depth from the ground surface in order to include the lower Layer III, which is a rocky formation of Schist. This layer has very good mechanical properties and is expected to act as a limit for the ground settlements as well as for the stability of the excavation’s slopes.

A very important factor for the accuracy of the numerical analyses is the generation and quality of the

finite element mesh. For the performed two-dimensional analysis 6-Noded elements were used, and a very fine mesh was created. In specific, a total number of 4199 elements was generated with a total number of 9202 nodes. “Fig. 3” shows the finite element mesh, which is very fine near the excavation area where higher values of displacements are expected and coarser close to the model’s boundaries. In “Fig. 4” the finite element mesh of the performed numerical analyses in three (3) dimensions is also presented.

Along the y-axis (see “Fig. 1”), in which the excavation’s side equals to  $L=44.2\text{m}$ , the lateral borders of the numerical model are placed in distance approximately 75m from the excavation’s slope. For all three-dimensional analyses 10-Noded elements were selected and a very fine mesh was created. The mesh includes a total number of 109298 elements and a total number of 190755 nodes.

#### B. Pile Wall Characteristics

The pile wall is numerically simulated using plate elements. In three-dimensional analyses the equivalent thickness of the pile wall is  $d=0.49\text{m}$ . The equivalent thickness of the wall is calculated from equalizing the moment of inertia of the piles with the moment of inertia of the equivalent compact wall per meter in the out of plane direction. In specific, for the calculation of the equivalent wall’s thickness the following equation is used, where “D” is the piles’ diameter and “s” is their axial spacing:

$$d = \left(12(\pi D^4 / 64) / s\right)^{1/3} \quad (1)$$

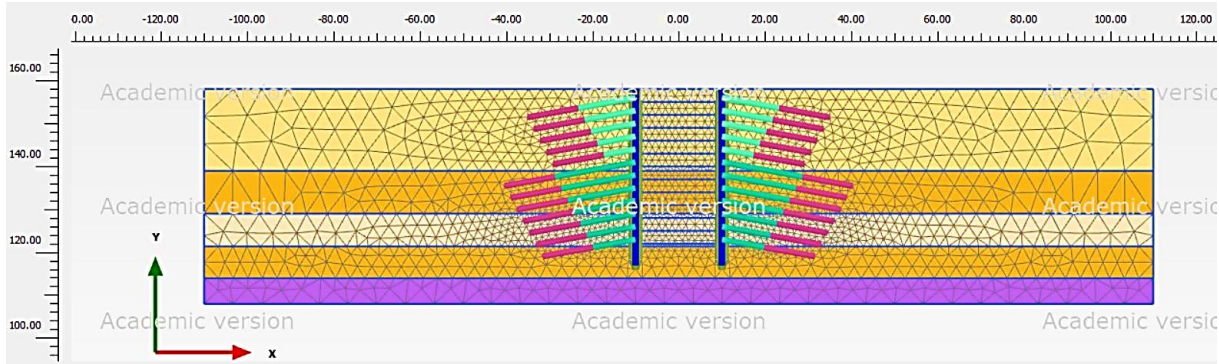


Figure 3. Finite element mesh of the two-dimensional numerical analysis.

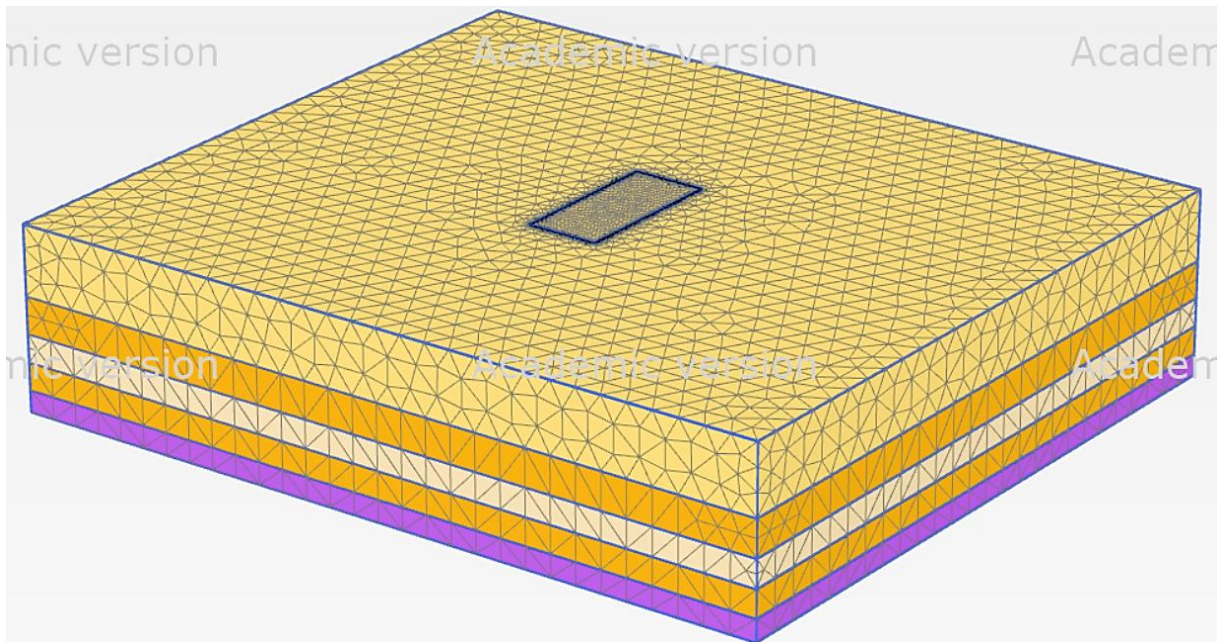


Figure 4. Finite element mesh of the three-dimensional numerical analyses.

Three-dimensional analyses are based on the assumption of the pile wall's behavior which is either isotropic or anisotropic. In case the wall is considered isotropic, the Young's Modulus is constant in all directions and equals to  $E=30\text{GPa}$ . In the contrary, for pile wall with structural anisotropy it is necessary to determine the Young's Modulus values  $E_1, E_2$  along the local axes 1 and 2 as well as the shear modulus values  $G_{12}, G_{23}, G_{13}$  of the wall. As the wall is constructed by an array of piles it develops very low values of axial forces  $N_2$ , shear forces  $Q_{12}, Q_{23}$  and bending moments  $M_{12}, M_{22}$ . This fact is reasonable because the piles are only connected in the direction of local axis 2 with shotcrete of small thickness. However, the anisotropic wall has high values of axial forces  $N_1$ , shear forces  $Q_{13}$  and bending moments  $M_{11}$ . In order to take the abovementioned data into consideration in the numerical analyses, the necessary input parameters of the anisotropic wall are determined using the following equations:

$$E_1 \approx E = 30\text{GPa} \quad (2)$$

$$E_2 = E_1 / 20 = 1.5\text{GPa} \quad (3)$$

$$G_{13} = EA_{13} / (2d(1+\nu)) \quad (4)$$

$$G_{12} = G_{23} = G_{13} / 20 \quad (5)$$

In equations (2) and (4),  $E$  is the Young's Modulus,  $d$  is the equivalent thickness of the pile wall and  $\nu$  is the Poisson ratio. As the piles are constructed with reinforced concrete, the Young's Modulus is considered  $E=30\text{GPa}$  and the Poisson ratio equals to  $\nu=0.2$ . The area of the cross section  $A_{13}$  activated during shear along the plane 1-3 is equal to the pile's area divided by the axial spacing.

### C. Numerical Simulation of the Construction Sequence

Three-dimensional numerical analyses with uniform excavation in the out of plane direction have the same construction phases as the two-dimensional analysis. Initially, geostatic stresses are calculated and the pile wall with its interfaces is activated.

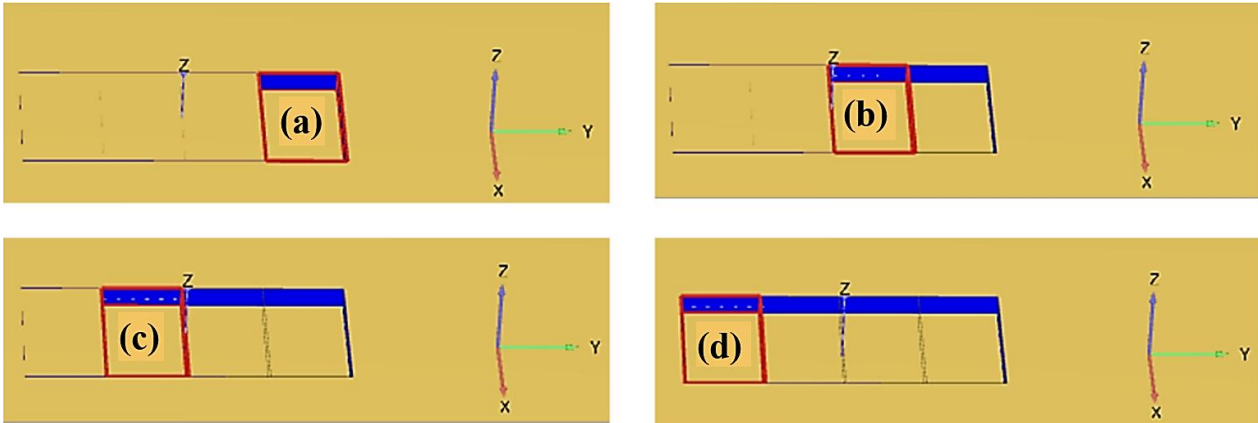


Figure 5. Excavation in stages (a), (b), (c) and (d) in the out of plane direction y-y.

Then the excavation phases are simulated, and the ground anchors are installed and pre-stressed. In each excavation phase the anchors of the previous phase are constructed and in that way the excavation is not simultaneous with the construction of the supporting measures. As a result, the design is conservative as the excavation is temporarily supported only by the pile wall for a depth of 4m that is the sum of each phase's depth (3m) and the vertical distance of the anchors (1m) from the excavation phase's final elevation. After the completion of all excavation phases and before the installation of the last row of anchors, a stability analysis is performed, in order to obtain the minimum stability safety factor.

Numerical analyses in three (3) dimensions with staged construction in the out of plane direction y-y approach the actual construction sequence more accurately, as the excavation of each phase in the field is carried out in stages. The stages (a), (b), (c) and (d) of excavation in the out of plane direction y-y are presented in "Fig. 5". After the excavation of each stage the pre-stressed anchors of the previous stage are constructed. In that way, the excavation's sides do not remain unsupported in the entire surface of the excavation ( $B \times L = 20.0 \times 44.2\text{m}$ ) but in smaller areas depending on the number of stages in the out of plane direction y-y. In specific, for two (2) excavation stages along y-axis the maximum area that remains unsupported until the construction of pre-stressed anchors equals to:  $B \times L/2 = 20.0 \times 22.1\text{m}$ . In case of four (4) excavation stages the maximum area that remains temporarily unsupported equals to:  $B \times L/4 = 20.0 \times 11.05\text{m}$ .

#### IV. RESULTS

The results of all numerical analyses are presented in the following diagrams. "Fig. 6" shows the vertical displacements developed at the ground surface for the cross section that passes from the middle of the excavation's long side, i.e., at  $L/2$  from the excavation's corner (in y direction). The abovementioned cross section is less affected by the excavations borders and for that reason has the maximum settlements.

From "Fig. 6" it is concluded that numerical analyses in three (3) directions lead to more favorable results in terms of vertical displacements, as the maximum ground

settlement calculated in three-dimensional analyses equals to 2.5mm and is significantly reduced in comparison with the maximum settlement calculated in two-dimensional analysis which is equal to 5.5mm.

Additionally, "Fig. 7" presents the distribution with depth of (a) wall lateral displacement  $U_x$ , (b) axial force  $N_1$  and (c) bending moment  $M_{11}$  for the cross section that passes from the middle point of the excavation's long side ( $L=44.2\text{m}$ ).

The distribution of the pile wall's lateral displacement with depth is graphically presented in "Fig. 7(a)". It is observed that the lateral displacement gets its maximum value at 32m depth which is approximately 4m above the excavation's bottom. Up to 28m depth (80% of the excavation's total depth) the curve of two-dimensional analysis has higher values of lateral displacement compared with those of three-dimensional analyses. However, it is notable that the maximum lateral displacement ( $\approx 1.7\text{cm}$ ) is calculated from three-dimensional analysis with anisotropic pile wall and uniform excavation in the out of plane direction y-y.

"Fig. 7(b)" presents the diagram of axial force  $N_1$  at the pile wall in correlation with depth from the ground surface. The axial force is maximum at the excavation's bottom. According to the diagrams, it is concluded that three-dimensional analyses lead to lower values of axial forces at the pile wall in comparison with two-dimensional analyses. Especially, for numerical analyses with consideration of the wall's structural anisotropy it is observed that the maximum axial force is significantly reduced from the one calculated from two-dimensional analysis.

The wall's bending moment  $M_{11}$  is presented in "Fig. 7(c)". The maximum bending moment for all presented curves is approximately at 33m depth, whereas the minimum bending moment is developed at approximately 37m depth. Three-dimensional analysis with isotropic wall has the maximum bending moment which is reasonable because the isotropic wall develops the smaller lateral displacements (see "Fig. 7(a)"). In the contrary, the anisotropic wall has the largest lateral displacement and therefore the lower values of bending moment.

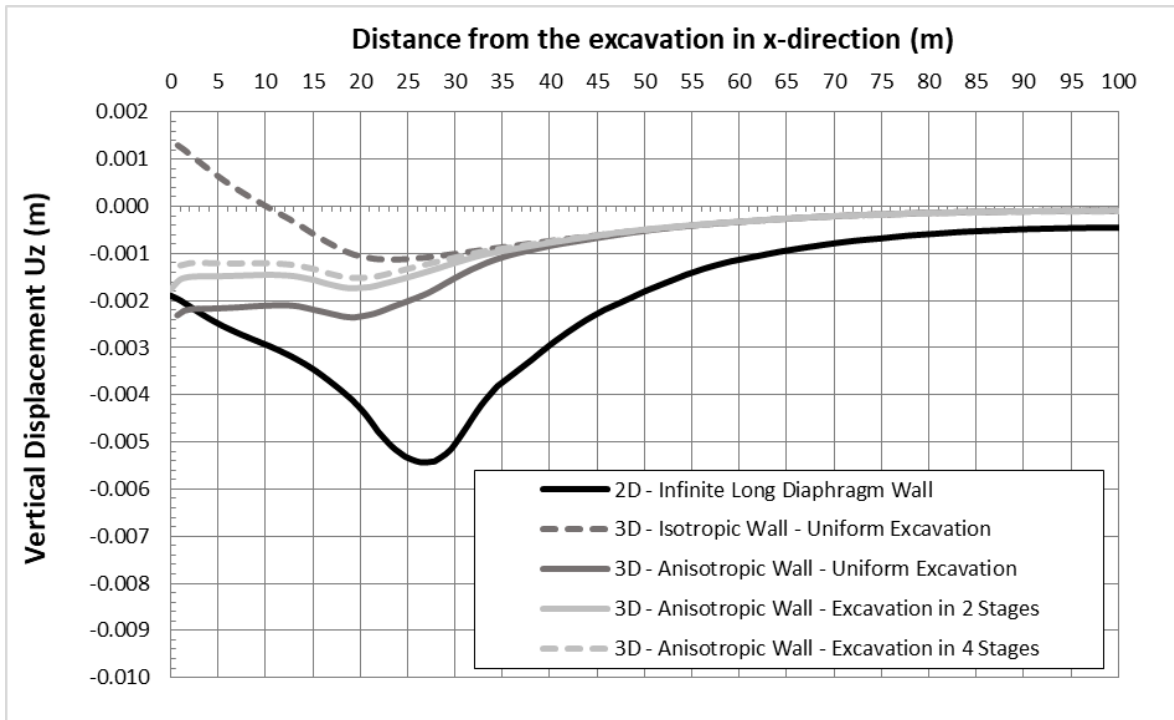


Figure 6. Correlation of vertical displacements at the ground surface with distance from the excavation's edge. The examined cross section passes from the middle point of the excavation's long side (with  $L=44.2\text{m}$ ).

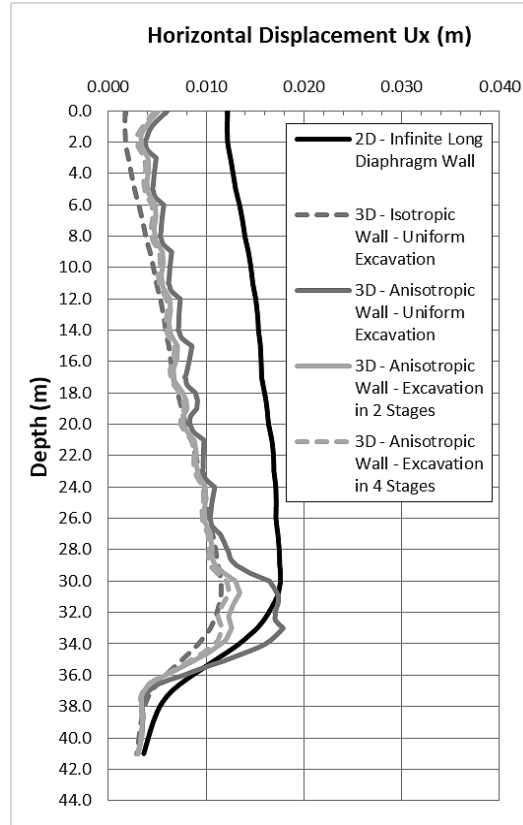
The comparison of three-dimensional analyses is presented for the cross sections that pass from the middle of the long side ( $L=44.2\text{m}$ ) and the short side ( $B=20\text{m}$ ) of the excavation, respectively. "Fig. 8" presents the distribution of wall's lateral displacement with depth for the analysis with uniform excavation in the out of plane direction considering isotropic and anisotropic wall as well as the analyses for anisotropic pile wall and excavation in two (2) and four (4) stages in direction of  $y$ -axis. In "Fig. 9" the distribution of axial force  $N_1$  with depth is presented for all the above-mentioned numerical analyses. From all diagrams of "Fig. 8" it is observed that the wall's lateral displacement is 25-35% higher in the longer side of the excavation. Moreover, the wall's structural anisotropy (see "Fig. 9(b)") leads to significantly higher values of lateral displacement in comparison with isotropic wall (see "Fig. 9(a)"). In the contrary, axial forces  $N_1$  developed at the anisotropic wall are reduced from those of the isotropic wall.

## V. CONCLUSION

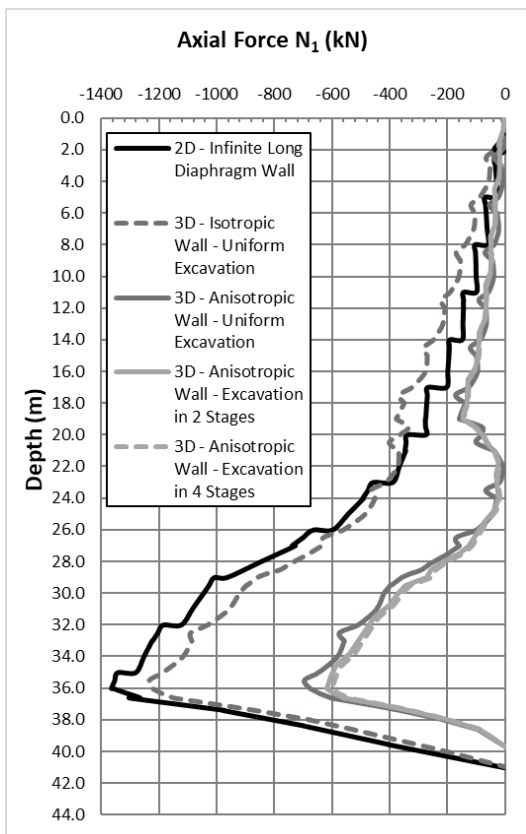
From the comparison between two-dimensional and three-dimensional analyses the following conclusions were conducted:

- for both two-dimensional and three-dimensional analyses with isotropic pile wall it is observed that the settlement of the ground surface becomes maximum at approximately 25m from the excavation's edge,

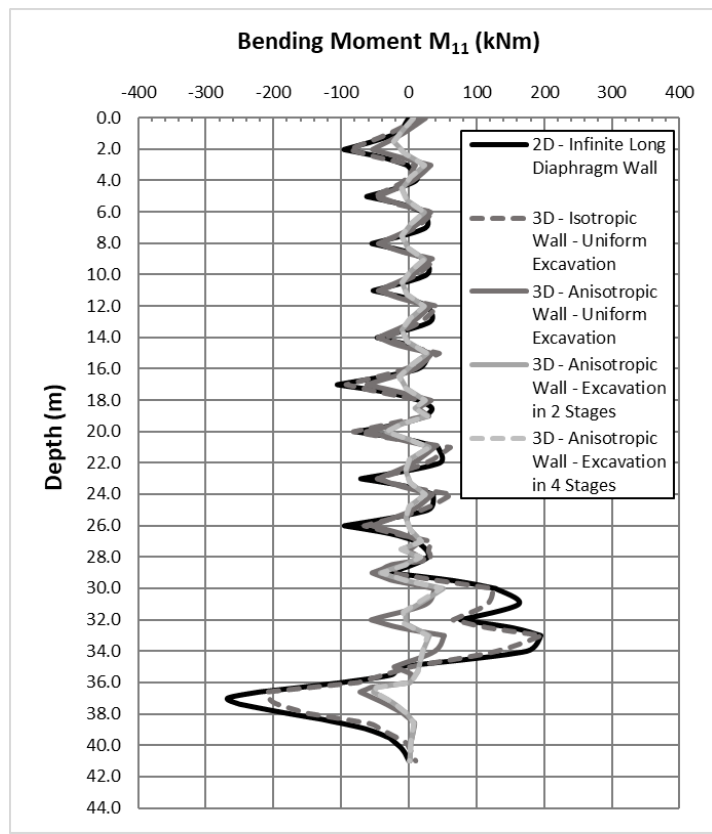
- the maximum lateral displacement of the wall is calculated from the numerical analysis in three (3) dimensions with anisotropic wall and uniform excavation in the out of plane direction  $y$ - $y$ ,
- the axial force becomes maximum at the excavation's bottom which is at 36m depth from the ground surface,
- the maximum bending moment is developed at the depth of 33m, whereas the minimum bending moment is developed at the depth of 37m,
- it is generally observed that when the diaphragm wall has large deformation, then its internal structural forces are lower, whereas when the wall has small deformation, then its internal structural forces become higher,
- the lateral displacement of the wall developed at the cross section of the excavation's long side is increased in comparison with the one developed at the cross section of the excavation's that passes from the middle of the short side,
- the internal structural forces ( $N_1$ ,  $M_{11}$ ,  $Q_{13}$ ) at the cross section of the excavation's long side is similar to those at the excavation's short side,
- three-dimensional analysis with isotropic diaphragm wall gives closer results to two-dimensional analysis regarding the internal structural forces developed at the wall,
- the assumption of staged construction in the out of plane direction  $y$ - $y$  improves slightly the results in terms of displacements and internal structural forces.



(a)



(b)



(c)

Figure 7. Distribution with depth of (a) lateral displacement  $U_x$ , (b) axial force  $N_1$  and (c) bending moment  $M_{11}$  for the cross section that passes from the middle point of the excavation's long side (with  $L=44.2m$ ).

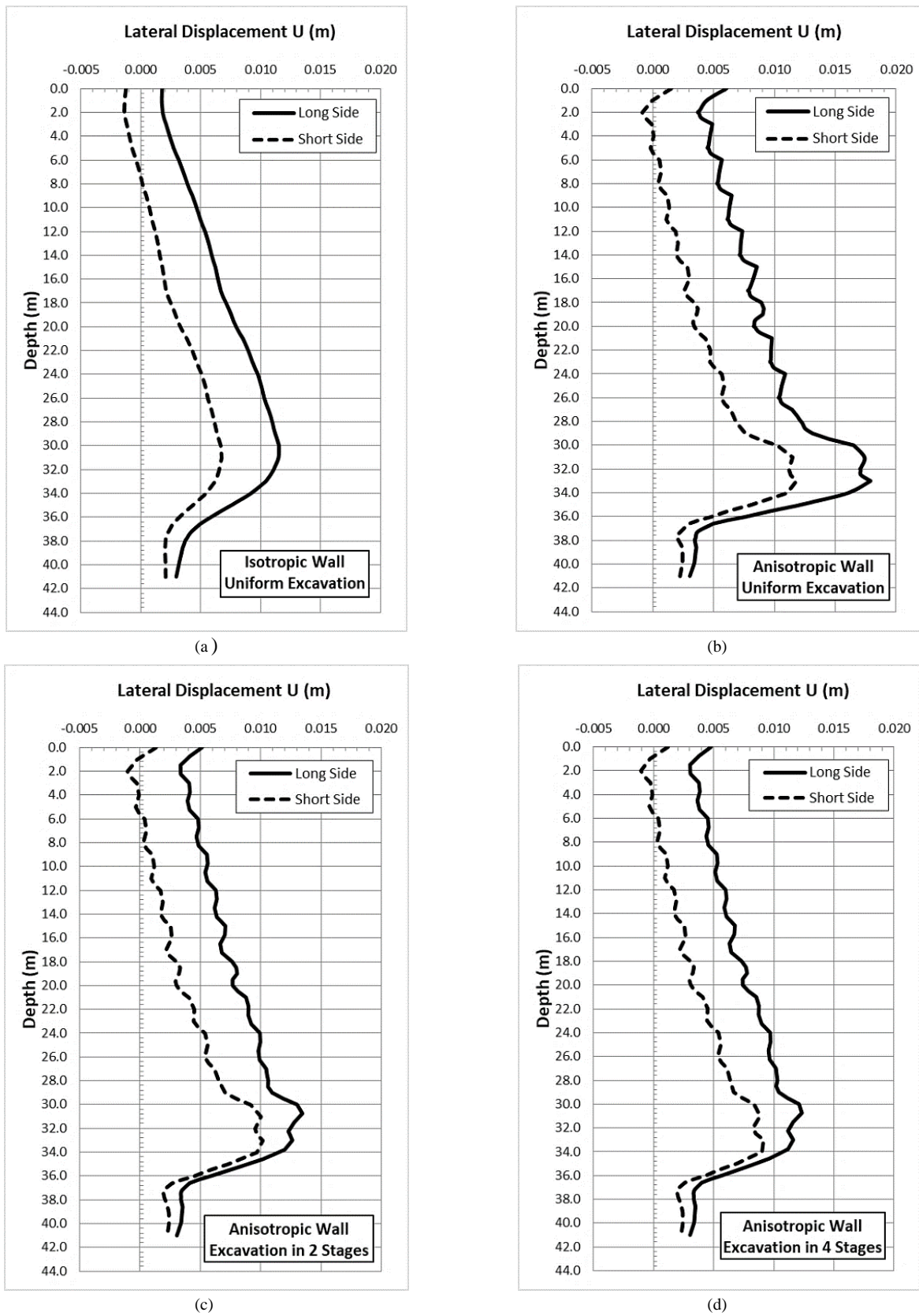


Figure 8. Comparative diagrams of numerical analyses for the cross sections that pass from the middle points of the short and long side of the excavation, respectively. Distribution of lateral displacement  $U$  with depth for (a) isotropic wall, (b) anisotropic wall & uniform excavation, (c) anisotropic wall & excavation in 2 stages and (d) anisotropic wall & excavation in 4 stages.

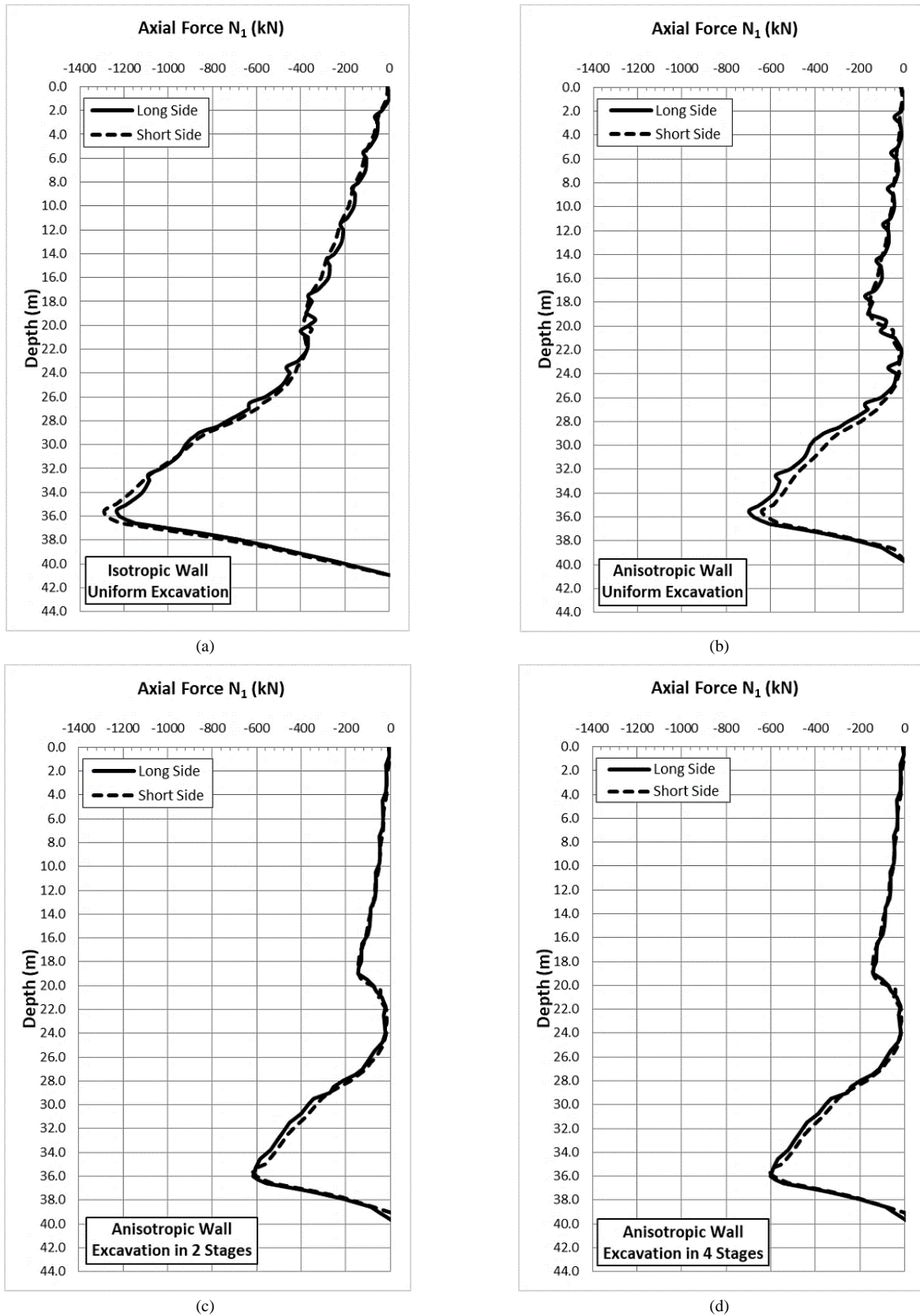


Figure 9. Comparative diagrams of numerical analyses for the cross sections that pass from the middle points of the short and long side of the excavation, respectively. Distribution of axial force  $N_1$  with depth for (a) isotropic wall, (b) anisotropic wall & uniform excavation, (c) anisotropic wall & excavation in 2 stages and (d) anisotropic wall & excavation in 4 stages.

#### CONFLICT OF INTEREST

The authors declare no conflict of interest.

#### AUTHOR CONTRIBUTIONS

Conceptualization, M.S. and N.G.; methodology, M.S. and N.G.; software, M.S.; validation, M.S. and N.G.; formal analysis, M.S.; investigation, M.S.; resources, M.S. and N.G.; data curation, M.S.; writing—original draft preparation, M.S.; writing—review and editing, N.G.; visualization, M.S. and N.G.; supervision, N.G.;

#### REFERENCES

- [1] C. Y. Ou, D. C. Chiou, T. S. W., "Three-dimensional finite element analysis of deep excavations," *Journal of Geotechnical Engineering*, vol. 122(May), pp. 337–345, 1996.
- [2] C. Cheng and S. Likitlersuang, "Underground excavation behaviour in Bangkok using three-dimensional finite element method," *Computers and Geotechnics*, Elsevier, 2018, vol. 95, October 2017, pp. 68–81.
- [3] R. J. Finno, M. Asce, J. T. Blackburn, A. M. Asce, J. F. Roboski, A. M. Asce, "Three-dimensional effects for supported excavations in clay," *Journal of Geotechnical and Geoenvironmental Engineering*, vol. 133(January), pp. 30–36, 2007.
- [4] A. Hefny, M. E. Al-atroush, M. Abualkhair, M. J. Alnuaimi, "Three-dimensional response of the supported-deep excavation system: Case study of a large scale underground metro station," *Geosciences*, 2020.

Copyright © 2022 by the authors. This is an open access article distributed under the Creative Commons Attribution License ([CC BY-NC-ND 4.0](https://creativecommons.org/licenses/by-nc-nd/4.0/)), which permits use, distribution and reproduction in any medium, provided that the article is properly cited, the use is non-commercial and no modifications or adaptations are made.



**Maria Spanea** is a graduate Civil Engineer of the National Technical University of Athens (NTUA). She dedicated the last year of her undergraduate studies in NTUA, in the elaboration of a very high level of Diploma thesis entitled "Evolution of Earthquake-induced Liquefaction on Sand Deposits with Intermediate "Weak" Layer". Solid was the decision of the Three-Member Examination Board to give the mark of 10 (Excellent).

This research resulted in two (2) publications, one in the Proceedings of an International Conference (*Computational Methods in Structural Dynamics and Earthquake Engineering-2021*) and one in the Proceedings of a National Conference (*Hellenic Conference in Geotechnical Engineering-2019*). She continued her studies in the Interdepartmental Postgraduate Programme of the School of Civil Engineering of NTUA entitled "Analysis and Design of Earthquake Resistant Structures". She dedicated the last year of her postgraduate studies in NTUA, in the elaboration of a very high level of Master thesis entitled "Numerical Analysis of Deep Excavation in Two (2) and Three (3) Dimensions".



**Nikos Gerolymos** is an Associate Professor in the School of Civil Engineering at the National Technical University of Athens. He teaches and conducts research in the area of Soil Mechanics, Computational Geotechnics, Soil-Structure Interaction and Earthquake Geotechnical Engineering. In his career, Prof Gerolymos has co-authored over than 170 scientific publications delivered invited lectures and general reports in international and national conferences. He has served as a reviewer of scientific articles for more than 60 international journals, many international / national conferences and research proposals, and as an editorial board member of 4 peer-reviewed scientific journals. He has worked as a main researcher in 25 research projects in Greece and the EU and contributed to the supervision of 10 PhD dissertations and about 70 Master and Diploma theses. Maintaining a strong link with the industry, he has over than 25 years of professional experience in consultancy services for major public engineering projects (energy, transportation and infrastructure) in Greece and worldwide. His methodology regarding the seismic analysis of caisson foundations has been applied in the design of several megabridges (e.g., the highway channel across the Qiongzhou Strait in China and the Dhubri-Phulbari bridge in Assam, India), while his constitutive soil model for sand behaviour and liquefaction-related deformation, designated as Ta-Ger (Tasiopoulou and Gerolymos, 2016), has been widely recognized among the most versatile models for 3D cyclic loading analysis at very large number of cycles and has been extensively used in the design of major projects including bridges, LNG tanks, offshore wind farms and port facilities. His teaching work received the highest grade in the evaluation of courses and tutors by the students of the Civil Engineering School during the 2014-2015 academic year. He awarded the distinction of Outstanding Reviewer for "Soil Dynamics and Earthquake Engineer" in the same year. He is a member of the National Standardization Body of Greece (ELOT) since 2019.